

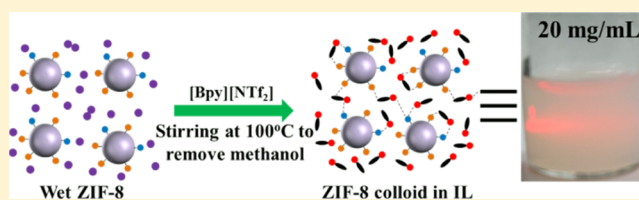
Porous Liquid: A Stable ZIF-8 Colloid in Ionic Liquid with Permanent Porosity

Shengjun Liu,^{†,§} Jiandang Liu,^{‡,§} Xudong Hou,[†] Tingting Xu,[†] Jing Tong,[†] Junxiang Zhang,[†] Bangjiao Ye,[‡] and Bo Liu^{*,†}

[†]Department of Chemistry and [‡]State Key Laboratory of Particle Detection and Electronics, University of Science and Technology of China, Hefei, Anhui 230026, P. R. China

S Supporting Information

ABSTRACT: We reported an example of metal–organic framework (MOF)-based porous liquid by dispersing ZIF-8 ($\{Zn(mim)_2\}$, mim = 2-methylimidazole) nanocrystallites in ionic liquid (IL) of $[Bpy][NTf_2]$ (*N*-butyl pyridinium bis(trifluoromethyl sulfonyl)imide). Two essential challenges, stable colloid formation and porosity retention, have been overcome to prepare MOF-based porous liquid. Preventing ZIF-8 nanocrystals from aggregation before dispersing is vital to form a stable ZIF-8 colloid in IL via enhancing the interaction between ZIF-8 and IL. The resultant ZIF-8– $[Bpy][NTf_2]$ colloid is able to be stable over months without precipitating. $[Bpy][NTf_2]$ with larger ion sizes cannot occupy pores in ZIF-8, leaving the ZIF-8 cage empty for enabling access by guest molecules. The porosity of this porous liquid system was verified by positron (e^+) annihilation lifetime spectroscopy and I_2 adsorption in ZIF-8 in the colloid. MOF-based porous liquids could provide a new material platform for liquid-bed-based gas separations.



INTRODUCTION

Porous materials including carbon materials,¹ zeolites,² polymers of intrinsic microporosity,³ metal–organic frameworks (MOFs),^{4,5} and so forth are important in both science and industry because of their high surface area and hence their application as absorbents, especially in adsorption and separation. In general, porosity is associated with materials in the solid state.⁶ In contrast, only liquid produces transient intermolecular cavities because of the molecular thermal movement. Nevertheless, such types of cavities are too small to be accessed by guest molecules.⁷ Even though porous solids possess numerous advantages, porous liquid is highly desired owing to its unique advantages in comparison with solid counterparts in terms of easy transport and facile process for thin-film fabrication and so forth. For example, most mature technology for CO_2 capture is liquid-based solvents (alkyl amines) rather than highly porous solid MOFs or other porous materials.⁸ James and co-workers first proposed the concept of porous liquids (more precisely, liquids with permanent microporosity).⁹ Accordingly, three types of porous liquid were put forward including type I: neat liquid with cavities; type II: rigid molecules having intrinsic cavities dissolved in solvents, and type III: porous frameworks suspending in solvents.¹⁰ Some poly-ionic liquids (ILs) showing permanent porosity belongs to type I porous liquid.^{11,12} Very recently, Coudert and co-workers reported that melting ZIF-4 in the liquid state retained chemical configuration, coordinative bonding modes, and porosity of the parent crystalline framework.¹³ Surface-modified hollow silica spheres with organosilane species also led to a type I porous liquid at room temperature.¹⁴ Multiple

alkylation of rigid organic cages rendered the transformation from porous crystal to type I porous liquid.¹⁵ Organic cages with intrinsic cavities dissolved in solvents are classified into type II, in which solvent molecules have larger molecular dimensions than cavity sizes.¹⁶

In the case of porous solids dispersing in solvents, porous solids tend to participate and solvent molecules are apt to occupy the pores in solids, which make it challenging to form type III porous liquid. Stable dispersion of microporous frameworks in organic solvents has been demonstrated via surface modification;^{17,18} however, there is no related porosity of the system reported in the reports. Until recently, Dai and co-workers reported an example of type III porous liquids based on rational coupling of microporous framework nanoparticles as porous hosts with a bulky IL as the fluid media.¹⁹

EXPERIMENTAL SECTION

Materials and Instrumentation. All chemicals were from commercial sources and used without further purification: zinc nitrate hexahydrate (99%), methanol (AR), *N,N*-dimethylformamide (AR), ethyl alcohol (AR), and chloroform (AR) were purchased from Sinopharm Chemical Reagent Co., Ltd; 2-methyl-imidazole (98%) and iodine (99.8%) were purchased from Macklin; and *N*-butyl pyridinium bis(trifluoromethyl sulfonyl)imide ($[Bpy][NTf_2]$) was purchased from Lanzhou Greenchem ILS, LICP. CAS. China. Powder X-ray diffraction (PXRD) patterns were collected on a Rigaku MiniFlex 600 X-ray diffractometer with $Cu K\alpha$ radiation ($\lambda = 1.54178 \text{ \AA}$). N_2 , CH_4 , and

Received: December 29, 2017

Revised: March 6, 2018

Published: March 6, 2018

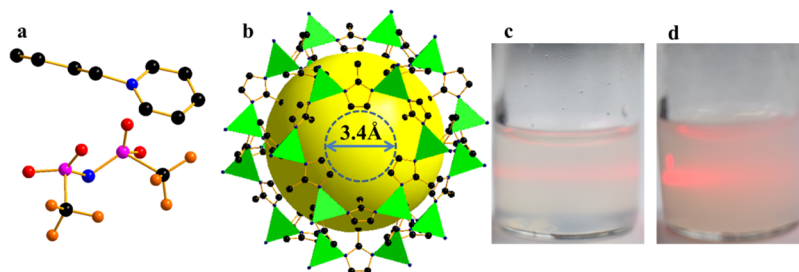


Figure 1. Molecular structure of (a) [Bpy][NTf₂] and (b) crystal structure of ZIF-8 (yellow sphere represents the cavity within the framework). (Zinc, carbon, nitrogen, oxygen, sulfur, and fluorine atoms are shown in green, black, blue, red, pink, and orange, respectively.) (H atoms are omitted for clarity); the photos of (c) 5 and (d) 20 mg ZIF-8 colloids in 1 mL of [Bpy][NTf₂] with the Tyndall effect.

CO₂ sorption isotherms were measured on a BEL sorp-max machine, BEL, Japan. An air-dried ZIF-8 sample was activated in vacuum at 100 °C for 12 h. N₂ sorption isotherms were recorded at 77 K. CO₂ and CH₄ adsorption were recorded at 298 K. Thermogravimetric (TG) analyses were performed on a TGA Q500 integration thermal analyzer from 25 to 600 °C at a heating rate of 10 °C min⁻¹ in N₂ atmosphere. ¹H and ¹³C NMR spectra were recorded by an Avance AV 400 spectrometer at an ambient temperature. The positron lifetime experiments were carried out with a fast–slow coincidence ORTEC system with a time resolution of ~230 ps full width at half-maximum. A 5 mCi source of ²²Na was sandwiched between two identical samples, and the total count was 2 million.

Experimental Section. Preparation of ZIF-8 Nanocrystals. The synthesis of ZIF-8 nanocrystals is based on a previous procedure.²⁰ A solution of Zn(NO₃)₂·6H₂O (0.738 g, 2.48 mmol) in methanol (50 mL) was rapidly added to a solution of 2-methylimidazole (1.643 g, 19.99 mmol) in methanol (50 mL) at 50 °C under stirring at 500 rpm. The mixture was stirred for 1 h at 50 °C. The precipitate was washed with methanol three times and collected by centrifugation (10 000 rpm, 5 min). The dried ZIF-8 powder was obtained, followed by drying in air. In contrast, the sample without drying step was denoted as wet ZIF-8.

Preparation of Dried ZIF-8 in ILs. The dried ZIF-8 powder (5 mg) was added into 1 mL of [Bpy][NTf₂] and treated with ultrasonication for 10 min.

Preparation of a Stable ZIF-8 Colloid in ILs. The wet ZIF-8 (5 or 20 mg) was added into 1 mL of [Bpy][NTf₂] and then stirred at 100 °C under vacuum to remove methanol. ZIF-8 was collected from the ZIF-8–IL stable colloid by centrifugation, washed with methanol, and dried in air for PXRD measurement to test the ZIF-8 stability in IL.

¹H/¹³C NMR (CDCl₃) Measurements. The wet ZIF-8 (5 or 20 mg) was dispersed into 1 mL of [Bpy][NTf₂]. The colloid of 100 μL was added into 500 μL of CDCl₃ for NMR measurement and denoted as ZIF-8–CH₃OH–IL. The colloid was treated at 100 °C under vacuum for 12 h, aiming to remove CH₃OH. The treated colloid (100 μL) was added into 500 μL of CDCl₃ for NMR measurement and denoted as ZIF-8–IL.

Loading Iodine into ZIF-8–MeOH and ZIF-8–IL Colloid. I₂–ZIF-8–IL colloid: iodine (20 mg) was added into a stable ZIF-8–[Bpy][NTf₂] colloid (1 mL, 20 mg mL⁻¹) at room temperature.

I₂–ZIF-8 (Methanol). ZIF-8 (20 mg) was dispersed in iodine–methanol solutions (1 mL, 20 mg mL⁻¹) at room temperature.

Measurement of CO₂/CH₄ Adsorption in [Bpy][NTf₂] (1 mL) and ZIF-8 (20 mg) in [Bpy][NTf₂] (1 mL). We adopt an isochoric technique^{16,21,22} to determine CO₂/CH₄ adsorption in [Bpy][NTf₂] (1 mL) and ZIF-8–[Bpy][NTf₂] colloid (20 mg mL⁻¹). In this technique, a known quantity of gaseous solute is placed in contact with a gravimetrically determined quantity of degassed solvent at a constant temperature inside an accurately known volume. When thermodynamic equilibrium is attained at a given temperature, the pressure drop is used to calculate the quantity of gas absorbed by adsorbents.

The experimental setup is represented in Figure S1. The whole setup was maintained inside a water bath to control the temperature (±0.1 K). The pressure is monitored in real time using a computer

algorithm. The samples are degassed by keeping it under a primary vacuum (approximately 1 Pa) at 100 °C for 12 h before measurement.

Positron Annihilation. Positron (e⁺) annihilation lifetime spectroscopy (PALS) measurements were performed using a fast–fast coincidence setup.²³ As a positron source, radioactive ²²Na (in the form of NaCl, in aqueous solution) was applied between two film cuts of 4 × 4 mm² to obtain a so-called sandwich geometry. To meet the penetration depth of positrons emitted by ²²Na, samples were prepared to a resulting thickness of 1 mm each side, typically one piece of 1 mm on each side. Because of this condition, surface contributions and contributions from annihilation in air could be neglected. Almost simultaneous to the emission of a positron from the decaying ²²Na, a 1.27 MeV γ-quantum is emitted, serving as a “start” signal for lifetime measurement. The “stop” signal is given by one of the two 511 keV γ-quanta emitted from positron annihilation. A multichannel analyzer recorded the spectra consisting of 2 × 10⁶ of such events for the samples. Spectra analysis was performed with the discrete lifetime analysis routine LIFETIME 9 similar to previous investigations.²³

Positron lifetime spectrum $N(t)$ is given by

$$N(t) = \sum_{i=1}^{k+1} I_i \exp\left(-\frac{t}{\tau_i}\right) \quad (1)$$

k denotes different types of defects that contribute to the positron capture and are related to the $k + 1$ component in the PALS spectra with the lifetime τ_i and intensity I_i . We divided the three components, that is, studied two types of defects, so $k = 2$.²⁴

All spectra were evaluated with discrete lifetime components, of which the longer one is assigned to the pore of the sample.

RESULTS AND DISCUSSION

MOFs represent the most promising porous solids benefiting from their tunable structures and pores.^{25–27} Some one- and two-dimensional MOFs can be dissolved, more exactly, dispersed in solvents; however, there are no accessible pores available in such systems.²⁸ To develop MOF-based porous liquid (type III), we have to identify the solvents that will not occupy the pores in MOFs. On the other hand, to form stable colloids, interaction between MOF particles and solvents must overcome the gravity (or floatage) of MOF particles in the solvents. Herein, we demonstrated a MOF-based porous liquid using [Bpy][NTf₂] and ZIF-8 ({Zn(mim)₂}, mim = 2-methylimidazole)^{29,30} as a solvent and a porous solid, respectively (Figure 1a,b). ZIF-8 nanocrystallites dispersed in [Bpy][NTf₂] gave rise to a stable colloid with permanent microporosity for I₂ adsorption (Figure 1c,d).

ILs as a new type of solvent are featured with negligible volatility, nonflammability, high thermal and chemical stability, and high ionic conductivity. ILs have shown promising applications as new green solvents for chemical reactions, catalysis, and electrolytes in electrochemistry.^{31,32} IL can be

hosted in MOFs,³³ for example, [BMI]Cl (BMI = 1-butyl-3-methylimidazolium) in MIL-101 due to the matchable ions and pore sizes.³⁴ Different from molecular solvents, ILs is composed of cations and anions. Either component with a larger size than the pore size in MOFs will prevent ILs from accessing the pores in MOFs because of the strong electrostatic attraction between cations and anions.

Nanosized ZIF-8 crystallites were synthesized according to the procedures in literature.²⁰ ZIF-8 has a pore opening size of 0.34 nm and a cavity size of 1.2 nm (Figure 1b),^{29,30} which allow most solvents to access. Therefore, common solvents, such as water, alcohol, *N,N*-dimethylformamide, chloroform, and so forth, are not suitable for our target. As observed, direct dispersion of ZIF-8 nanoparticles in these solvents resulted in complete precipitation over time (Figure S2). We selected IL [Bpy][NTf₂] as a solvent for ZIF-8 dispersion because dimension of the [Bpy] cation (ca. 12.1 × 7.2 × 5.5 Å³) is larger than the pore opening size of ZIF-8 (Figure 1a), which hinders the occupation of cavities by the solvent. Nevertheless, directly dispersing dried ZIF-8 powder into [Bpy][NTf₂] led to ZIF-8 floating in ILs (Figure S3). The dried ZIF-8 powder was obtained by centrifuging reaction solution and washing with methanol, followed by drying in air. In contrast, the ZIF-8 sample without drying step was hereinafter denoted as wet ZIF-8.

The particle sizes of dried ZIF-8 were evaluated to be ca. 19 nm by Scherrer equation from PXRD data (Figure S4). This is consistent with scanning electron microscopy (SEM) observation (Figure 2), where particle size distribution of ZIF-8 nanocrystallites was estimated to be ca. 20 nm (inset of Figure 2c). As seen from SEM images, even the particles are small, the

particles seriously aggregated together for dried ZIF-8 (Figure 2a,b). On the surface of nanosized ZIF-8, there are abundant amount of reactive Zn²⁺ ions and 2-methyl-imidazole species. When ZIF-8 nanoparticles get in contact, superficial Zn²⁺ and 2-methyl-imidazole from adjacent particles could bond each other for aggregation. It should be pointed out that ZIF-8 was synthesized at 50 °C. In addition, the drying process was carried out at a higher temperature (100 °C). Therefore, it is thermodynamically favorable for superficial Zn²⁺ and 2-methyl-imidazole bonding in drying process. The aggregation effect is not reversible owing to the strong bonding effect. The dispersing forces, including van der Waals' force, electrostatic interaction, and so forth, mainly depends on the interaction between ILs and ZIF-8 surface species.^{35–38} The aggregation will greatly decrease this interaction because it reduces the external surface area and thus superficial groups of ZIF-8. To avoid the aggregation, we directly mixed the reaction solution for nanosized ZIF-8 synthesis and [Bpy][NTf₂] and then removed methanol by heating under vacuum. In this way, we could prepare a stable ZIF-8 colloid in [Bpy][NTf₂] (Figure S5). Nevertheless, the reaction mixture inevitably contains some unreacted precursors (Zn(NO₃)₂ and 2-methyl-imidazole).

The above dispersion procedure is further modified accordingly. The ZIF-8 reaction solution was centrifuged and washed with methanol three times to completely remove unreacted species. Then, the collected wet ZIF-8 nanocrystallites (without drying step) was obtained and dispersed in [Bpy][NTf₂]. After removing the residual methanol by heating at 100 °C under vacuum, ZIF-8 (5, even 20 mg) can be well-dispersed in 1 mL of [Bpy][NTf₂]. By comparing the ¹H and ¹³C NMR spectra before and after the methanol removal step, we can clearly conclude that methanol has been completely removed from the ZIF-8-[Bpy][NTf₂] colloid (Figure S6). ZIF-8 of 5 or 20 mg dispersing in 1 mL of [Bpy][NTf₂] gave rise to obvious Tyndall effect, and no sedimentation can be observed over months as tested (Figure 1c,d). The ZIF-8-[Bpy][NTf₂] colloid remained stable after 7 months (Figure S7). Wet ZIF-8 cannot form stable colloids in [BPy][BF₄] (*N*-butylpyridinium tetrafluoroborate) and [HPy][NTf₂] (Figure S8). As observed from SEM images, the aggregation degree is much reduced for this wet ZIF-8 in comparison with that of dried ZIF-8 (Figure 2a,c). This implied that methanol in the wet ZIF-8 sample efficiently restrained the aggregation because of its solvation effect (Figure 2d). Hence, the interaction between ZIF-8 and IL can be greatly strengthened to support ZIF-8 dispersing in IL. We added methanol into the stable colloid (5 mg mL⁻¹) and separated ZIF-8 by centrifuging. The SEM image as shown in Figure 2e clearly indicated that ZIF-8 nanoparticles were surrounded by IL. It is worth to note that IL cannot be removed in a high vacuum chamber in SEM measurement because of its extremely low vapor pressure. This explained why the stable colloid can be formed from the less aggregated wet ZIF-8 sample.

Surface engineering has been widely applied to modify the surface properties of nanoparticles, for example, binding soft or flexible polymers with the nanoparticle surface to form self-suspended fluids of nanoparticles.^{39–42} Very recently, Talapin and co-workers demonstrated that surface-bound solvent ions produced long-ranged charge-density oscillations in the molten salt around solute particles (including metals, semiconductors, rare-earth compounds, and magnetic materials) and prevented their aggregation for stable colloid formation. First, organic

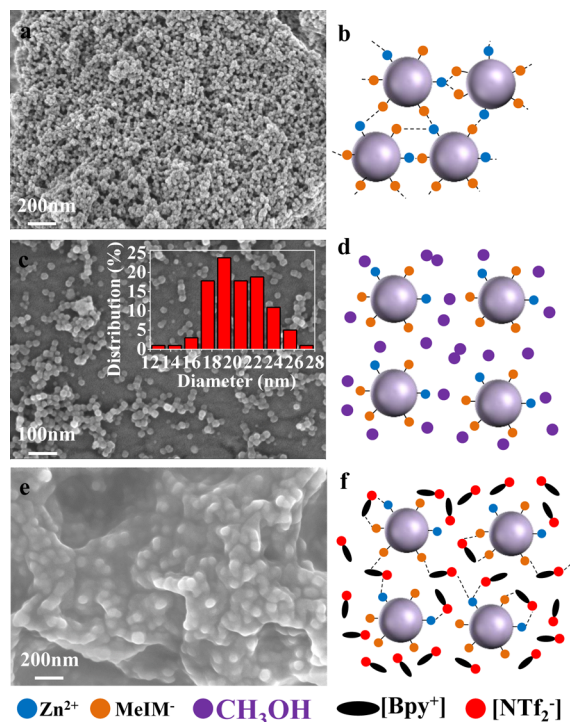


Figure 2. SEM images of (a) dried, (c) wet ZIF-8 (inset, size distribution analysis for the ZIF-8 particles), and (e) ZIF-8 recovered from the stable ZIF-8-[Bpy][NTf₂] colloid. Structural illustration of (b) dried ZIF-8, (d) wet ZIF-8, and (f) stable ZIF-8-[Bpy][NTf₂] colloid.

ligands on the surface of nanoparticles can be effectively solvated with ILs to form stable colloids. Second, hydrophilic ILs do not effectively solvate nanoparticle ligands but have sufficient nucleophilicity and affinity to the surface of nanoparticle.⁴³ In this work, surface groups of nanosized ZIF-8 interacting with ions in IL prevented the aggregation and helped the formation of stable colloid. It should be emphasized that preaggregation before dispersing must be avoided because aggregation is an irreversible process. In the case of ZIF-8 nanoparticles, wetting ZIF-8 with methanol has been proven to be efficient for this purpose, as demonstrated above (Figure 2c,d).

Confirmed by NMR data as mentioned above, there is no methanol existing in the ZIF-8–IL colloid after heating under vacuum. Therefore, we can exclude the possibility of CH₃OH occupation in pores of ZIF-8. Predicted from molecular dimensions of [Bpy][NTf₂] and pore opening size of ZIF-8 (Figure 1), we expect that ions in IL are restrained from accessing the cavities in ZIF-8. Thus, ZIF-8 in [Bpy][NTf₂] will keep its original porosity. N₂ sorption data implies that ZIF-8 recovered from the ZIF-8–IL colloid exhibited the almost same adsorption behavior as pristine ZIF-8 (Figure 3). However, this

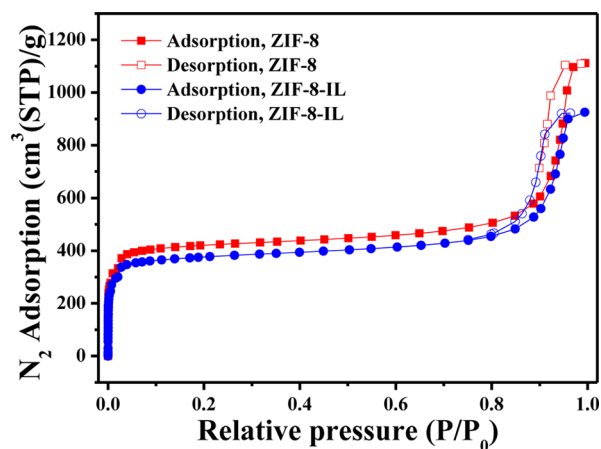


Figure 3. N₂ adsorption and desorption isotherms of pristine ZIF-8 (red) and ZIF-8 recovered from the stable colloid (blue).

is not the direct evidence of porosity existing in the ZIF-8–IL colloid. It is well-studied that ILs are good solvents to dissolve a

wide range of materials.^{44–46} Hence, it is difficult to directly probe the porosity of ZIF-8 in IL using gas adsorption because of good solubility of gas species in IL and relatively low content of ZIF-8 in IL (20 mg mL⁻¹ equals to 1.4 wt % ZIF-8 in IL). Our experiments indicated that CO₂ and CH₄ adsorption in [Bpy][NTf₂] (1 mL) and ZIF-8 (20 mg) in [Bpy][NTf₂] (1 mL) show no obvious difference (Figures 4 and S1, see details in the Supporting Information).

To confirm whether pores of ZIF-8 in ILs are empty or not, PALS spectra were collected over samples of ZIF-8, [Bpy][NTf₂], and ZIF-8–[Bpy][NTf₂] (Table 1, Figures S9 and S10, see details in the Supporting Information). PALS technology is a well-established technique to study empty pore in materials.^{16,46–49} In principle, the positrons emitted from the positron source, such as ²²Na, will annihilate through the interaction with electrons in materials. In case voids are available, positrons will reside in voids and annihilate less rapidly than in the bulk of the material. The positron lifetime can be correlated with the average pore diameter in the material by a well-established model.^{47–50} Thus, by comparing the positron lifetimes observed in ZIF-8, [Bpy][NTf₂], and ZIF-8–[Bpy][NTf₂] colloid, we could draw the information about the porosity of ZIF-8 in the colloid.

The positron lifetime parameters of ZIF-8, [Bpy][NTf₂], and ZIF-8–[Bpy][NTf₂] colloid are listed in Table 1. The short lifetime ($\tau_1 = 0.294$ ns) is contributed by the ligand of ZIF-8, and the two longer components ($\tau_2 = 0.545$ ns and $\tau_3 = 2.418$ ns) are due to positron annihilation in the small pore and the larger pore in ZIF-8, respectively.^{29,30} Two lifetimes of 0.418 and 3.169 ns were detected in the [Bpy][NTf₂] sample. In addition, the ZIF-8–IL colloid consists of three lifetimes, in which τ_1 (0.419 ns) and τ_2 (3.169 ns) matched with the lifetimes of [Bpy][NTf₂] and τ_3 is ascribed to ZIF-8 in the colloid. In comparison with [Bpy][NTf₂], the ZIF-8–[Bpy][NTf₂] colloid shows one more positron lifetime ($\tau_3 = 0.721$ ns), which nearly equals to the weighted average lifetime of ZIF-8 ($\tau_m = 0.748$ ns, Table 1). Therefore, it is reasonable to conclude from PALS data that ZIF-8 is empty in [Bpy][NTf₂].

To further verify the porosity of ZIF-8 in [Bpy][NTf₂], iodine was selected as a probe molecule as I₂ adsorption in ZIF-8 has been demonstrated previously.^{51–54} I₂ dissolved in the ZIF-8–[Bpy][NTf₂] (20 mg mL⁻¹) colloid can be adsorbed by ZIF-8 (Figure 5a). The I₂@ZIF-8 composite can be collected by centrifuging from the mixture of I₂–ZIF-8–IL. As a control

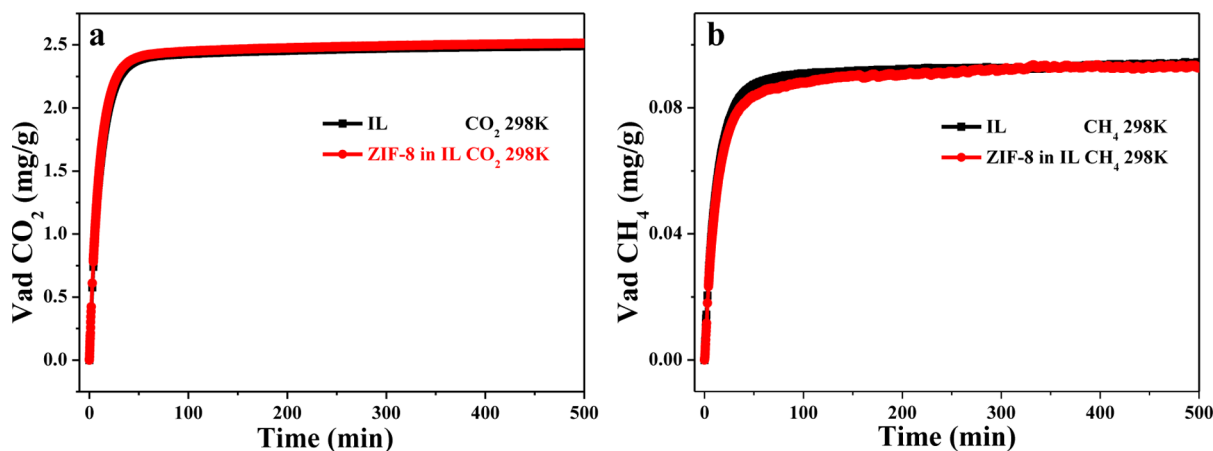


Figure 4. (a) CO₂ and (b) CH₄ adsorption in [Bpy][NTf₂] (1 mL) and ZIF-8 (20 mg) in [Bpy][NTf₂] (1 mL) at 298 K.

Table 1. Positron Lifetime Parameters of ZIF-8, [Bpy][NTf₂], and Stable ZIF-8-[Bpy][NTf₂] Colloid^a

sample	τ_1 (ns)	τ_2 (ns)	τ_3 (ns)	I_1 (%)	I_2 (%)	I_3 (%)
ZIF-8	0.294 ± 0.006	0.545 ± 0.017	2.418 ± 0.011	55.70 ± 1.90	26.00 ± 2.10	18.30 ± 0.68
IL	0.418 ± 0.001	3.169 ± 0.016		91.93 ± 0.03	8.07 ± 0.03	
ZIF-8-IL	0.419 ± 0.008	3.169 ± 0.085	0.721 ± 0.078	90.71 ± 0.31	7.84 ± 0.05	1.46 ± 0.34

^a τ : positron (e⁺) annihilation lifetime and I : intensity of lifetime.

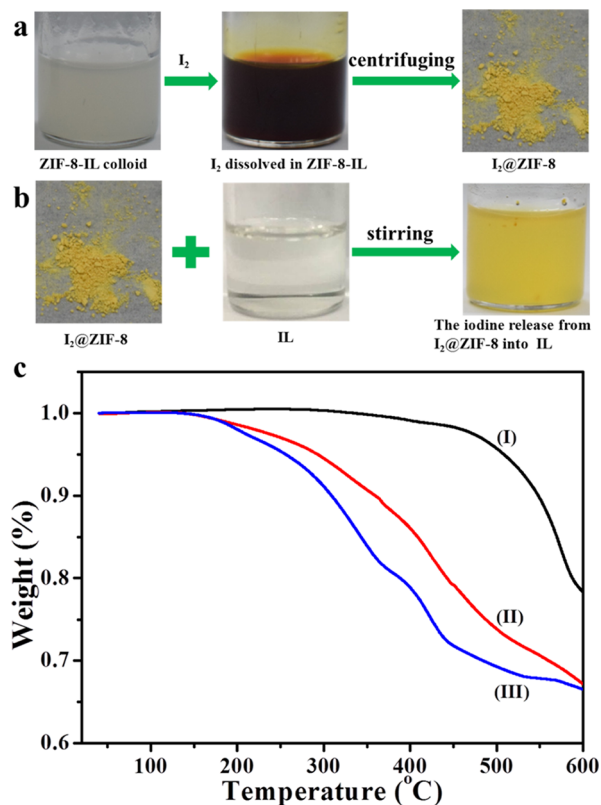


Figure 5. (a) I₂ adsorption by ZIF-8 in the ZIF-8-[Bpy][NTf₂] colloid (20 mg mL⁻¹); (b) I₂ release from I₂@ZIF-8 into [Bpy][NTf₂]; and (c) TG analyses of (I) pristine ZIF-8, (II) I₂@ZIF-8 obtained from I₂-MeOH solution, and (III) I₂@ZIF-8 obtained from the ZIF-8-IL colloid.

experiment, we dispersed the composite of I₂@ZIF-8 in [Bpy][NTf₂]; I₂ released from ZIF-8 into IL was also observed (Figure 5b). It has been demonstrated that I₂ can be adsorbed in cavities and on the surface of ZIF-8.^{51,52} I₂ adsorbed on the surface can be easily removed by subliming because of weak van der Waals' force before 200 °C, whereas I₂ in cages requires higher temperature (>200 °C) to be eliminated. TG analyses indicated that the pristine ZIF-8 framework was stable up to 400 °C in an N₂ atmosphere (Figure 5c(I)). We compared TG behavior of I₂ adsorbed ZIF-8 from the I₂-methanol solution and the ZIF-8-IL colloid (Figure 5c(II),(III)). Methanol can be preremoved by heating at 100 °C under vacuum as demonstrated above. As seen from TG curves, there is no weight loss before 100 °C. Weight losses between 100 and 200 °C are ascribed to I₂ adsorbed on the surface (1.38 and 1.97 wt %, respectively for both samples). I₂ adsorbed in the cavity of ZIF-8 was determined to be 12.72 and 13.66 wt %, respectively, as calculated from the weight loss between 200 and 400 °C. I₂ adsorption/release experiments clearly revealed that ZIF-8 in the colloid preserved its porosity as pristine ZIF-8.

NMR experiments have shown no methanol in the ZIF-8-IL colloid, whereas [Bpy][NTf₂] is larger than pore opening sizes of ZIF-8. Therefore, we could exclude the possibility of methanol and [Bpy][NTf₂] occupation in pores of ZIF-8. Associated with PALS results and I₂ adsorption/release experiment, we confirmed that we successfully prepared the stable ZIF-8-IL colloid with permanent porosity.

CONCLUSIONS

In summary, we demonstrated a MOF-based porous liquid by dispersing ZIF-8 nanocrystallites in [Bpy][NTf₂]. The key of success to prepare a stable ZIF-8 colloid in IL is to increase the interaction between the MOF surface and IL. To avoid preaggregation of ZIF-8, we adopted wet ZIF-8 rather than dried powder in IL. Solvent (methanol) surrounding ZIF-8 is an effective approach to prevent ZIF-8 from aggregating before dispersing. The resultant ZIF-8 colloid in ILs can be stable over months without sedimentation. Importantly, ZIF-8 dispersed in [Bpy][NTf₂] preserved its porosity as pristine ZIF-8, as proved by I₂ adsorption/release experiments in [Bpy][NTf₂]. PALS study also revealed that ZIF-8 maintained its porosity in ILs. Considering the abundant amount of MOFs and ILs, MOF-based porous liquid could be infinite with potential applications toward liquid-bed-based gas separations.

ASSOCIATED CONTENT

Supporting Information

The Supporting Information is available free of charge on the ACS Publications website at DOI: 10.1021/acs.langmuir.7b04212.

Photos, PXRD patterns, ¹H and ¹³C NMR, gas adsorption apparatus, and PALS measurement setup (PDF)

AUTHOR INFORMATION

Corresponding Author

*E-mail: liuchem@ustc.edu.cn.

ORCID

Bo Liu: 0000-0002-1150-3709

Author Contributions

[§]S.L. and J.L. contributed equally.

Notes

The authors declare no competing financial interest.

ACKNOWLEDGMENTS

We gratefully acknowledge the financial support from National Natural Science Foundation of China (NSFC, 21571167 and 51502282), Chinese Academy of Sciences, the Fundamental Research Funds for the Central Universities (WK2060190053), and Anhui Province Natural Science Foundation (1608085MB28).

REFERENCES

- (1) Zhu, C.; Li, H.; Fu, S.; Du, D.; Lin, Y. Highly efficient nonprecious metal catalysts towards oxygen reduction reaction based on three-dimensional porous carbon nanostructures. *Chem. Soc. Rev.* **2016**, *45*, 517–531.
- (2) Wei, Y.; Parmentier, T. E.; de Jong, K. P.; Zečević, J. Tailoring and visualizing the pore architecture of hierarchical zeolites. *Chem. Soc. Rev.* **2015**, *44*, 7234–7261.
- (3) Hartmann, M.; Schwieger, W. Hierarchically-structured porous materials: from basic understanding to applications. *Chem. Soc. Rev.* **2016**, *45*, 3311–3312.
- (4) Bai, Y.; Dou, Y.; Xie, L.-H.; Rutledge, W.; Li, J.-R.; Zhou, H.-C. Zr-based metal–organic frameworks: design, synthesis, structure, and applications. *Chem. Soc. Rev.* **2016**, *45*, 2327–2367.
- (5) Schoedel, A.; Li, M.; Li, D.; O’Keeffe, M.; Yaghi, O. M. Structures of Metal–Organic Frameworks with Rod Secondary Building Units. *Chem. Rev.* **2016**, *116*, 12466–12535.
- (6) Romm, F. *Microporous Media: Synthesis, Properties, and Modeling*; CRC Press, 2004.
- (7) Pohorille, A.; Pratt, L. R. Cavities in molecular liquids and the theory of hydrophobic solubilities. *J. Am. Chem. Soc.* **1990**, *112*, 5066–5074.
- (8) Lepaumier, H.; Martin, S.; Picq, D.; Delfort, B.; Carrette, P.-L. New Amines for CO₂ Capture. III. Effect of Alkyl Chain Length between Amine Functions on Polyamines Degradation. *Ind. Eng. Chem. Res.* **2010**, *49*, 4553–4560.
- (9) O’Reilly, N.; Giri, N.; James, S. L. Porous liquids. *Chem.—Eur. J.* **2007**, *13*, 3020–3025.
- (10) Yamada, M.; Arai, M.; Kurihara, M.; Sakamoto, M.; Miyake, M. Synthesis and isolation of cobalt hexacyanoferrate/chromate metal coordination nanopolymers stabilized by alkylamino ligand with metal elemental control. *J. Am. Chem. Soc.* **2004**, *126*, 9482–9483.
- (11) Lee, J. S.; Luo, H.; Baker, G. A.; Dai, S. Cation cross-linked ionic liquids as anion-exchange materials. *Chem. Mater.* **2009**, *21*, 4756–4758.
- (12) Zhang, S.; Dokko, K.; Watanabe, M. Porous ionic liquids: synthesis and application. *Chem. Sci.* **2015**, *6*, 3684–3691.
- (13) Gaillac, R.; Pullumbi, P.; Beyer, K. A.; Chapman, K. W.; Keen, D. A.; Bennett, T. D.; Coudert, F.-X. Liquid metal–organic frameworks. *Nat. Mater.* **2017**, *16*, 1149–1154.
- (14) Zhang, J.; Chai, S.-H.; Qiao, Z.-A.; Mahurin, S. M.; Chen, J.; Fang, Y.; Wan, S.; Nelson, K.; Zhang, P.; Dai, S. Porous liquids: a promising class of media for gas separation. *Angew. Chem., Int. Ed.* **2015**, *54*, 932–936.
- (15) Giri, N.; Davidson, C. E.; Melaugh, G.; Del Pópolo, M. G.; Jones, J. T. A.; Hasell, T.; Cooper, A. I.; Horton, P. N.; Hursthouse, M. B.; James, S. L. Alkylated organic cages: from porous crystals to neat liquids. *Chem. Sci.* **2012**, *3*, 2153–2157.
- (16) Giri, N.; Del Pópolo, M. G.; Melaugh, G.; Greenaway, R. L.; Rätzke, K.; Koschine, T.; Pison, L.; Gomes, M. F. C.; Cooper, A. I.; James, S. L. Liquids with permanent porosity. *Nature* **2015**, *527*, 216–220.
- (17) Yamada, M.; Arai, M.; Kurihara, M.; Sakamoto, M.; Miyake, M. Synthesis and isolation of cobalt hexacyanoferrate/chromate metal coordination nanopolymers stabilized by alkylamino ligand with metal elemental control. *J. Am. Chem. Soc.* **2004**, *126*, 9482–9483.
- (18) Devaux, A.; Popović, Z.; Bossart, O.; De Cola, L.; Kunzmann, A.; Calzaferri, G. Solubilisation of dye-loaded zeolite L nanocrystals. *Microporous Mesoporous Mater.* **2006**, *90*, 69–72.
- (19) Shan, W.; Fulvio, P. F.; Kong, L.; Schott, J. A.; Do-Thanh, C.-L.; Tian, T.; Hu, X.; Mahurin, S. M.; Xing, H.; Dai, S. New Class of Type III Porous Liquids: A Promising Platform for Rational Adjustment of Gas Sorption Behavior. *ACS Appl. Mater. Interfaces* **2018**, *10*, 32–36.
- (20) Tsai, C.-W.; Langner, E. H. G. The effect of synthesis temperature on the particle size of nano-ZIF-8. *Microporous Mesoporous Mater.* **2016**, *221*, 8–13.
- (21) Jacquemin, J.; Gomes, M. F. C.; Husson, P.; Majer, V. Solubility of carbon dioxide, ethane, methane, oxygen, nitrogen, hydrogen, argon, and carbon monoxide in 1-butyl-3-methylimidazolium tetrafluoroborate between temperatures 283 K and 343 K and at pressures close to atmospheric. *J. Chem. Thermodyn.* **2006**, *38*, 490–502.
- (22) Husson-Borg, P.; Majer, V.; Gomes, M. F. C. Solubilities of Oxygen and Carbon Dioxide in Butyl Methyl Imidazolium Tetrafluoroborate as a Function of Temperature and at Pressures Close to Atmospheric Pressure. *J. Chem. Eng. Data* **2003**, *48*, 480–485.
- (23) Ye, B.; Kasugai, Y.; Ikeda, Y.; Fan, Y.; Zhou, X.; Du, J.; Han, R. The sputtering of radioactive recoil nuclides induced by fast neutron. *J. Appl. Phys.* **2000**, *87*, 2581–2586.
- (24) Oleiwi, M. H.; Talib, T. M. Study Positron Lifetime Spectrum with High Resolution Effect and Lifetime Effects. *Int. J. Appl. Eng. Res.* **2017**, *12*, 14854–14857.
- (25) Long, J. R.; Yaghi, O. M. The pervasive chemistry of metal–organic frameworks. *Chem. Soc. Rev.* **2009**, *38*, 1213–1214.
- (26) Zhou, H.-C.; Long, J. R.; Yaghi, O. M. Introduction to metal–organic frameworks. *Chem. Rev.* **2012**, *112*, 673–674.
- (27) Yaghi, O. M. Reticular Chemistry—Construction, Properties, and Precision Reactions of Frameworks. *J. Am. Chem. Soc.* **2016**, *138*, 15507–15509.
- (28) Huang, Y.-B.; Wang, Q.; Liang, J.; Wang, X.; Cao, R. Soluble Metal-Nanoparticle-Decorated Porous Coordination Polymers for the Homogenization of Heterogeneous Catalysis. *J. Am. Chem. Soc.* **2016**, *138*, 10104–10107.
- (29) Huang, X.-C.; Lin, Y.-Y.; Zhang, J.-P.; Chen, X.-M. Ligand-Directed Strategy for Zeolite-Type Metal–Organic Frameworks: Zinc (II) Imidazolates with Unusual Zeolitic Topologies. *Angew. Chem., Int. Ed.* **2006**, *45*, 1557–1559.
- (30) Park, K. S.; Ni, Z.; Côté, A. P.; Choi, J. Y.; Huang, R. D.; Uribe-Romo, F. J.; Chae, H. K.; O’Keeffe, M.; Yaghi, O. M. Exceptional chemical and thermal stability of zeolitic imidazolate frameworks. *Proc. Natl. Acad. Sci. U.S.A.* **2006**, *103*, 10186–10191.
- (31) Zhang, Z.; Song, J.; Han, B. Catalytic transformation of lignocellulose into chemicals and fuel products in ionic liquids. *Chem. Rev.* **2017**, *117*, 6834–6880.
- (32) Wang, B.; Qin, L.; Mu, T.; Xue, Z.; Gao, G. Are Ionic Liquids Chemically Stable? *Chem. Rev.* **2017**, *117*, 7113–7131.
- (33) Fujie, K.; Kitagawa, H. Ionic liquid transported into metal–organic frameworks. *Coord. Chem. Rev.* **2016**, *307*, 382–390.
- (34) Khan, N. A.; Hasan, Z.; Jhung, S. H. Ionic Liquids Supported on Metal–Organic Frameworks: Remarkable Adsorbents for Adsorptive Desulfurization. *Chem.—Eur. J.* **2014**, *20*, 376–380.
- (35) Derjaguin, B.; Landau, L. Theory of the stability of strongly charged lyophobic sols and of the adhesion of strongly charged particles in solutions of electrolytes. *Acta Physicochim. URSS* **1941**, *194*, 633–662.
- (36) Overbeek, J. T. G. Interparticle forces in colloid science. *Powder Technol.* **1984**, *37*, 195–208.
- (37) Napper, D. H. Steric stabilization. *J. Colloid Interface Sci.* **1977**, *58*, 390–407.
- (38) Shrotri, S.; Somasundaran, P. Particle Deposition and Aggregation, Measurement, Modeling and Simulation. *Colloids Surf., A* **1997**, *125*, 93–94.
- (39) Bourlinos, A. B.; Herrera, R.; Chalkias, N.; Jiang, D. D.; Zhang, Q.; Archer, L. A.; Giannelis, E. P. Surface-functionalized nanoparticles with liquid-like behavior. *Adv. Mater.* **2005**, *17*, 234–237.
- (40) Rodriguez, R.; Herrera, R.; Archer, L. A.; Giannelis, E. P. Nanoscale ionic materials. *Adv. Mater.* **2008**, *20*, 4353–4358.
- (41) Ueno, K.; Inaba, A.; Kondoh, M.; Watanabe, M. Colloidal Stability of Bare and Polymer-Grafted Silica Nanoparticles in Ionic Liquids. *Langmuir* **2008**, *24*, 5253–5259.
- (42) Gao, J.; Ndong, R. S.; Shiflett, M. B.; Wagner, N. J. Creating Nanoparticle Stability in Ionic Liquid [C₄mim][BF₄] by Inducing Solvation Layering. *ACS Nano* **2015**, *9*, 3243–3253.
- (43) Zhang, H.; Dasbiswas, K.; Ludwig, N. B.; Han, G.; Lee, B.; Vaikuntanathan, S.; Talapin, D. V. Stable colloids in molten inorganic salts. *Nature* **2017**, *542*, 328–331.
- (44) Ueno, K.; Fukai, T.; Nagatsuka, T.; Yasuda, T.; Watanabe, M. Solubility of Poly(methyl methacrylate) in Ionic Liquids in Relation to Solvent Parameters. *Langmuir* **2014**, *30*, 3228–3235.

(45) Carneiro, A. P.; Rodríguez, O.; Macedo, E. A. Dissolution and fractionation of nut shells in ionic liquids. *Bioresour. Technol.* **2017**, *227*, 188–196.

(46) Zhang, T.; Schwedtmann, K.; Weigand, J. J.; Doert, T.; Ruck, M. Dissolution behaviour and activation of selenium in phosphonium based ionic liquids. *Chem. Commun.* **2017**, *53*, 7588–7591.

(47) Mogensen, O. E. *Positron Annihilation in Chemistry*; Springer Series in Chemical Physics 58; Springer, 1995.

(48) Jean, Y. C.; Van Horn, J. D.; Hung, W.-S.; Lee, K.-R. Perspective of positron annihilation spectroscopy in polymers. *Macromolecules* **2013**, *46*, 7133–7145.

(49) Li, C.; Zhao, B.; Zhou, B.; Qi, N.; Chen, Z.; Zhou, W. Effects of electrical conductivity on the formation and annihilation of positronium in porous materials. *Phys. Chem. Chem. Phys.* **2017**, *19*, 7659–7667.

(50) Zhou, W.; Chen, Z.; Oshima, N.; Ito, K.; O'Rourke, B. E.; Kuroda, R.; Suzuki, R.; Yanagishita, H.; Tsutsui, T.; Uedono, A.; Hayashizaki, N. In-situ characterization of free-volume holes in polymer thin films under controlled humidity conditions with an atmospheric positron probe microanalyzer. *Appl. Phys. Lett.* **2012**, *101*, 014102.

(51) Hughes, J. T.; Sava, D. F.; Nenoff, T. M.; Navrotsky, A. Thermochemical evidence for strong iodine chemisorption by ZIF-8. *J. Am. Chem. Soc.* **2013**, *135*, 16256–16259.

(52) Sava, D. F.; Rodriguez, M. A.; Chapman, K. W.; Chupas, P. J.; Greathouse, J. A.; Crozier, P. S.; Nenoff, T. M. Capture of volatile iodine, a gaseous fission product, by zeolitic imidazolate framework-8. *J. Am. Chem. Soc.* **2011**, *133*, 12398–12401.

(53) Chapman, K. W.; Sava, D. F.; Halder, G. J.; Chupas, P. J.; Nenoff, T. M. Trapping Guests within a Nanoporous Metal–Organic Framework through Pressure-Induced Amorphization. *J. Am. Chem. Soc.* **2011**, *133*, 18583–18585.

(54) Sava, D. F.; Garino, T. J.; Nenoff, T. M. Iodine confinement into metal–organic frameworks (MOFs): low-temperature sintering glasses to form novel glass composite material (GCM) alternative waste forms. *Ind. Eng. Chem. Res.* **2012**, *51*, 614–620.